ORIGINAL ARTICLE

Cerebral blood flow, amyloid burden, and cognition in cognitively normal individuals

Jarith L. Ebenau[1] · Denise Visser[2] · Sander C. J. Verfaillie[2] · Tessa Timmers[2] · Mardou S. S. A. van Leeuwenstijn[1] · Mara ten Kate[2] · Albert D. Windhorst[2] · Frederik Barkhof[2,3] · Philip Scheltens[1] · Niels D. Prins[1,4] · Ronald Boellaard[2] · Wiesje M. van der Flier[1,5] · Bart N. M. van Berckel[2]

Abstract

Purpose The role of cerebral blood flow (CBF) in the early stages of Alzheimer's disease is complex and largely unknown. We investigated cross-sectional and longitudinal associations between CBF, amyloid burden, and cognition, in cognitively normal individuals with subjective cognitive decline (SCD).

Methods We included 187 cognitively normal individuals with SCD from the SCIENCe project (65 ± 8 years, 39% F, MMSE 29 ± 1). Each underwent a dynamic (0–70 min) [^{18}F]florbetapir PET and T1-weighted MRI scan, enabling calculation of mean binding potential (BP$_{ND}$; specific amyloid binding) and R_1 (measure of relative (r)CBF). Eighty-three individuals underwent a second [^{18}F]florbetapir PET (2.6 ± 0.7 years). Participants annually underwent neuropsychological assessment (follow-up time 3.8 ± 3.1 years; number of observations $n = 774$).

Results A low baseline R_1 was associated with steeper decline on tests addressing memory, attention, and global cognition (range betas 0.01 to 0.27, $p < 0.05$). High BP$_{ND}$ was associated with steeper decline on tests covering all domains (range betas -0.004 to -0.70, $p < 0.05$). When both predictors were simultaneously added to the model, associations remained essentially unchanged. Additionally, we found longitudinal associations between R_1 and BP$_{ND}$. High baseline BP$_{ND}$ predicted decline over time in R_1 (all regions, range betas$_{BP \times time}$ -0.09 to -0.14, $p < 0.05$). Vice versa, low baseline R_1 predicted increase in BP$_{ND}$ in frontal, temporal, and composite ROIs over time (range betas$_{R1 \times time}$ -0.03 to -0.08, $p < 0.05$).

Conclusion Our results suggest that amyloid accumulation and decrease in rCBF are two parallel disease processes without a fixed order, both providing unique predictive information for cognitive decline and each process enhancing the other longitudinally.

Keywords Alzheimer's disease · Cerebral blood flow · Amyloid · PET · R_1

This article is part of the Topical Collection on Neurology

✉ Jarith L. Ebenau
  j.ebenau@amsterdamumc.nl

1 Alzheimer Centre, Department of Neurology, Amsterdam Neuroscience, Vrije Universiteit Amsterdam, Amsterdam UMC, De Boelelaan 1118, 1081 HZ Amsterdam, The Netherlands

2 Department of Radiology & Nuclear Medicine, Amsterdam Neuroscience, Vrije Universiteit Amsterdam, Amsterdam UMC, Amsterdam, The Netherlands

3 UCL Institutes of Neurology and Healthcare Engineering, London, UK

4 Brain Research Centre, Amsterdam, The Netherlands

5 Department of Epidemiology & Data Science, Vrije Universiteit Amsterdam, Amsterdam UMC, Amsterdam, The Netherlands

Introduction

Deposition of amyloid β (Aβ) into plaques is one of the main pathophysiological hallmarks of Alzheimer's disease (AD) and an important determinant of cognitive decline [1, 2].

Amyloid accumulation is thought to be the primary event in the pathogenesis of AD, initiating a series of events that ultimately result in neuronal damage and dementia [3, 4]. The process of amyloid accumulation starts decades before the onset of dementia, and amyloid plaques can already be present in cognitively normal individuals [5]. Although amyloid pathology is an important marker of AD, other pathological processes also play a role, such as tau pathology, neuroinflammation, and changes in cerebral blood flow (CBF). Indeed, CBF is shown to be abnormal in AD dementia and

relates to changes in brain glucose metabolism and synaptic failure [6–8]. Several studies using measures of CBF such as arterial spin labelling (ASL) MRI, early phase amyloid PET, or [^{15}O]H$_2$O PET found a lower CBF to be associated with advancing disease stage [9–14]. It is currently unclear how CBF and amyloid burden are interrelated, especially in the early stages of the disease, as previous studies provide conflicting results and are hampered by small sample sizes [12, 15–21]. In addition, most studies used a cross-sectional design, precluding the investigation of longitudinal trajectories. Only one study investigated CBF longitudinally and found both increases and decreases in CBF in amyloid-positive individuals [16]. CBF has furthermore been shown to be associated with cognition, but studies provide conflicting results and longitudinal studies are scarce [22–24].

Amyloid burden and CBF can be assessed simultaneously in vivo with dynamic [^{18}F]florbetapir PET scans. Dynamic scanning provides two unique parameters of interest: (i) binding potential (BP$_{ND}$), which is an exact quantification of specific binding to Aβ [25], and (ii) R_1, which represents the ratio between K_1 (the rate constant for ligand transfer from plasma to tissue) in the target region and the reference region, and which can be seen as a measure for relative CBF (rCBF) [10, 26, 27]. As a result, one [^{18}F]florbetapir PET scan provides quantitative information on both amyloid load and rCBF.

This study focused on cognitively normal individuals who experienced cognitive complaints. These individuals presented to a memory clinic which makes them a clinically relevant population to study early amyloid pathology and the role of rCBF in the development of AD pathology. We hypothesized that both high amyloid burden and low rCBF are related to cognitive decline. Since CBF seems to decline in advancing disease stages, we hypothesized that a higher baseline amyloid burden is related to a subsequent decline in rCBF. The aims of this study were (1) to assess the association between amyloid burden, rCBF, and cognitive decline over time and (2) to investigate the relationship between (rate of accumulation of) amyloid burden and (rate of change in) rCBF in a relatively large sample of cognitively normal individuals.

Material and methods

Population

We included 187 cognitively normal individuals from the SCIENCe cohort, which is part of the Amsterdam Dementia Cohort [28, 29]. All participants with available [^{18}F]florbetapir PET and MRI and available cognitive data were included. PET scans used in this study were acquired between 2015 and 2021. One hundred and seventy-five individuals were referred to the memory clinic by their general physician, a geriatrician, or a neurologist. All underwent an extensive standardized diagnostic work-up, including a neurological and neuropsychological examination, laboratory testing, and brain MRI, which was read by an experienced neuroradiologist. In a consensus meeting, individuals were categorized as having subjective cognitive decline when clinical and cognitive investigations were normal and criteria were not met for mild cognitive impairment (MCI) or dementia, nor for other neurological or psychiatric diseases that could be the cause of cognitive complaints. Participants were followed up annually, during which neuropsychological testing and clinical investigation were repeated. In addition, 12 participants were included via the Dutch Brain Research Registry (hersenonderzoek.nl). All experienced cognitive complaints in the absence of objective impairment and all received the same baseline work-up.

Image acquisition

PET scans were acquired on an Ingenuity TF PET-CT ($n = 140$) or a Gemini TF PET-CT ($n = 47$; Philips, Best, the Netherlands) scanner which were calibrated to each other. Dynamic PET scans of 90 min ($n = 140$) were obtained starting simultaneously with tracer injection of approximately 370 MBq [^{18}F]florbetapir. During the course of the study, we demonstrated that scan duration could be reduced without compromising the reliability of results [25]. Therefore, subsequent scans had a duration of 70 min ($n = 43$). The scan was terminated early in four instances due to participant-related issues (three after 60 min, one after 79 min). These scans were nonetheless included because quantification was reliable in these subjects with relatively low amyloid load [25].

Follow-up scans were available for $n = 83$ (44%) ($n = 17$ 90-min scan; $n = 66$ 70-min scan). Mean time between the two PET scans was 2.6 ± 0.7 years.

In addition, all individuals underwent structural MRI. The protocol included 3D T1-weighted images, 3D T2-weighted images, and 3D T2-weighted fluid-attenuated inversion-recovery (FLAIR) images [30].

Image analysis

Data were reconstructed while using standard LOR RAMLA reconstruction algorithm with corrections for scatter, random coincidences, attenuation, decay, and dead time. Images were reconstructed with a matrix size of $128 \times 128 \times 90$ and a voxel size of $2 \times 2 \times 2$ mm^3. Isotropic 3-dimensional T1-weighted MR images were co-registered to PET images using Vinci software (Max Planck Institute, Cologne, Germany). Next, regions of interest (ROIs) were defined on the co-registered MRI using the probabilistic Hammers brain

atlas in PVElab [31]. Receptor parametric mapping (RPM) was used to generate parametric BP_{ND} and R_1 images with cerebellar gray matter as a reference region using PPET [25, 32–34]. We calculated (volume weighted) mean cortical BP_{ND} and R_1 in the following (bilateral) ROIs: frontal, temporal, parietal, occipital, and a composite ROI consisting of orbitofrontal, temporal, parietal, anterior cingulate, posterior cingulate, and precuneus regions [35]. The difference in time between MRI and PET was generally within 1 year (median time difference 0.2 years (IQR $-0.5 - 0.5$)).

White matter hyperintensities were visually assessed using the Fazekas scale (range 0–3) [36]. Microbleeds were assessed on T2-weighted images and defined as small dot-like hypointense lesions. They were counted and dichotomized into absent (0) or present (≥ 1 microbleed). Scans were reviewed by a neuroradiologist.

Neuropsychological assessment

All participants underwent extensive standardized neuropsychological assessments [30]. For memory, we used the Visual Association Test version A (VAT-A) and the total immediate and delayed recall condition of the Dutch version of the Rey Auditory Verbal Learning Task (RAVLT). To assess language, we used category fluency (animals). For attention, we used the Trail Making Test A (TMT-A) and Stroop tasks I and II (naming and color naming). For executive functioning, we used the TMT-B and Stroop task III (color-word). For global cognition, we used the Mini-Mental State Examination (MMSE). Raw test scores for TMT and Stroop were log transformed, because data were right-skewed. Values were subsequently inverted, so that a lower score implies worse test performance for all tests. We used available test results of visits before as well as after the PET scan, in order to accurately estimate the cognitive slope [37]. This resulted in longitudinal cognitive data covering 3.8 ± 3.1 years. Concurrent time points were defined as the visit closest to the date of the baseline PET scan (median -0.19, IQR -0.41 to 0.00). In total, 774 neuropsychological investigations of 187 patients were available ($165 \geq 2$ visits, median 3).

Statistics

All analyses were performed in R version 4.0.3. For all analyses, BP_{ND} and R_1 were transformed into Z-scores, for comparability of effect sizes. Z-scores were based on baseline PET scans ($n = 187$). We used the false discovery rate (FDR) to correct for multiple testing, and FDR corrected p values < 0.05 were considered significant. We used linear mixed models (LMM) with time as determinant to estimate slopes for imaging measures and cognitive tests for the whole group.

First, we investigated the relationship between baseline R_1, baseline BP_{ND}, and cognitive test performance, using LMM. For this set of models, the composite ROI was used. Model 1 included R_1, time, and $R_1 \times$ time as predictors and cognitive test results as outcome. Separate models were run with different cognitive tests as outcome measure ($n = 10$ neuropsychological tests). Next, we repeated the analyses with BP_{ND} instead of R_1 as predictor (model 2). Then we included both R_1 and BP_{ND} as predictors in the model (predictors: R_1, BP_{ND}, time, $R_1 \times$ time, $BP_{ND} \times$ time; model 3). When we ran model 3, we tested whether there was an interaction between $R_1 \times BP_{ND} \times$ time for all neuropsychological tests. When this interaction term was significant, we provide the betas full model including the three-way interaction term. When the three-way interaction was not significant, it was removed from the model. All models were corrected for age, sex, education, and PET and MRI scanner type. Models included a random intercept, and a random slope if this improved the model fit, which was the case for RAVLT immediate, RAVLT delayed, Stroop II, Stroop III, and MMSE.

We then used LMM to assess the cross-sectional and longitudinal relationship between BP_{ND} and R_1. We first assessed the effect of baseline BP_{ND} on R_1. Model 1 included baseline BP_{ND}, time, and $BP_{ND} \times$ time as predictors, and R_1 as outcome (including baseline and follow-up R_1 values). Model 2 was additionally corrected for age, sex, and PET and MRI scanner type. In the models, "BP_{ND}" represents the effect of BP_{ND} on R_1, when time $= 0$. The interaction term "$BP_{ND} \times$ time" reflects the effect of BP_{ND} on annual change in R_1. We analyzed the associations in frontal, temporal, parietal, occipital, and composite regions separately, such that for each analysis, the ROI used for BP_{ND} was the same as the ROI used for R_1. Subsequently, we performed an additional set of analyses, where predictors and outcome were reversed so that baseline R_1, time, and $R_1 \times$ time were used as predictors, and longitudinal BP_{ND} as outcome. Models included a random intercept.

For visualization in the figures, we used tertiles to divide our sample based, on R_1 (low, intermediate, and high baseline R_1) and BP_{ND} (low, intermediate, and high baseline BP_{ND}).

Results

Demographics

Table 1 shows the baseline demographics of the sample. One hundred and eighty-seven individuals were on average 64.6 ± 7.6 years old, 74 (39%) were female, MMSE was 28.9 ± 1.2, and 69 (39%) were APOE4 carrier. Fazekas score and number of microbleeds were low. During follow-up, 13

Table 1 Baseline demographics

		Total $N = 187$	
Demographics	Age, mean $\pm$ SD	64.61 ± 7.61	
	Sex, n female (%)	73 (39.04%)	
	Education, median [IQR]	6 [5–6]	
	APOE4 carriership, n (%)	69 (39.20%)	
	Amyloid positivity, n (%)†	45 (24.06%)	
	Fazekas, mean $\pm$ SD	0.88 ± 0.79	
	Microbleeds, n (%)‡	32 (17.11%)	
	Clinical progression, n (%)¤	13 (6.95%)	
		Concurrent	Annual change
Amyloid burden	BP_{ND} frontal	0.18 (0.012)	0.02 (0.003)*
	BP_{ND} temporal	0.13 (0.009)	0.01 (0.002)*
	BP_{ND} parietal	0.21 (0.012)	0.01 (0.002)*
	BP_{ND} occipital	0.20 (0.009)	0.00 (0.002)
	BP_{ND} composite	0.17 (0.010)	0.01 (0.002)*
Relative cerebral blood flow	R_1 frontal	0.93 (0.004)	0.01 (0.002)*
	R_1 temporal	0.89 (0.004)	0.003 (0.001)*
	R_1 parietal	0.95 (0.004)	-0.003 (0.002)*
	R_1 occipital	0.98 (0.004)	-0.003 (0.002)
	R_1 composite	0.92 (0.004)	0.002 (0.010)
Neuropsychological tests	VAT-A	11.53 (0.053)	-0.04 (0.013)*
	RAVLT immediate	44.77 (0.594)	0.62 (0.150)*
	RAVLT delayed	8.99 (0.196)	0.11 (0.048)*
	Animal fluency	23.56 (0.364)	0.02 (0.061)
	TMT-A§	-3.47 (0.020)	-0.001 (0.003)
	TMT-B§	-4.32 (0.024)	-0.004 (0.003)
	Stroop I§	-3.75 (0.011)	0.002 (0.002)
	Stroop II§	-4.05 (0.012)	0.01 (0.002)*
	Stroop III§	-4.52 (0.016)	0.02 (0.003)*
	MMSE	28.76 (0.071)	0.05 (0.024)

Baseline demographics in the total sample. Data is presented as mean (SE) unless otherwise specified. Values for BP_{ND}, R_1, and cognitive test results do not represent the observed data but are obtained using linear mixed models with time as only predictor (intercept as concurrent value at time of baseline PET scan; beta associated with time as value for annual change). Annual change for BP_{ND} and R_1 is based on the subset with an available follow-up PET ($n = 83$)

*p value < 0.05

†Amyloid positivity as determined by visual assessment of baseline [18F]florbetapir PET

‡Values are dichotomized into 0 counts and ≥ 1 counts; n shown is number of participants with ≥ 1 count

§Values are log transformed and inverted such that a lower score implies a worse test result, complicating interpretation of values

¤Clinical progression to mild cognitive impairment $n = 9$, *AD* dementia $n = 2$, dementia with Lewy bodies $n = 1$, vascular dementia $n = 1$

BP_{ND} binding potential, *VAT* Visual Association Test, *RAVLT* Rey Auditory Verbal Learning Task, *TMT* Trail Making Test, *MMSE* Mini-Mental State Examination

individuals progressed to MCI or dementia (MCI $n = 9$, AD dementia $n = 2$, dementia with Lewy bodies $n = 1$, vascular dementia $n = 1$).

Eighty-three individuals underwent follow-up PET. Individuals in this subset were similar to the total sample in terms of baseline demographics. In this cognitively normal group, we found on average only very subtle changes over time. BP_{ND} increased over time in frontal, temporal, parietal, and composite regions, with the greatest change in the frontal region (beta 0.02 (SE 0.003)). On average, R_1 also

increased over time in frontal and temporal regions (0.01 (0.002); 0.003 (0.001)), but decreased subtly in the parietal region (-0.003 (0.002)). Baseline neuropsychological test scores were within age- and education-dependent norms. Over time and for the whole sample, we found a small improvement on RAVLT immediate, RAVLT delayed, Stroop II, and Stroop III, while the score on VAT-A became somewhat lower over time.

Relationship between BP_{ND}, R_1, and cognition

We first analyzed how both baseline PET markers were associated with cognitive performance (Table 2, Fig. 1). We did not find any cross-sectional associations between R_1 and any of the cognitive tests (model 1). By contrast, we found effects of R_1 on slope of several tests (p for interaction with time < 0.05). A lower baseline R_1 was associated with a worse trajectory for tests for memory (RAVLT immediate and delayed), attention (TMT-A), and global cognition (MMSE), but not for tests in other

cognitive domains. The results did not remain significant after correction for multiple testing. Next, we used baseline BP_{ND} as predictor in our models (model 2). We only found a cross-sectional association between a higher baseline BP_{ND} and a lower MMSE score. By contrast, we found effects of BP_{ND} on slope for a large number of tests. After correction for multiple testing, associations between BP_{ND} and cognitive slope remained significant for RAVLT immediate, RAVLT delayed, Animal Fluency, and Stroops I–III. When we simultaneously entered BP_{ND} and R_1 in model 3, results remained essentially unchanged. Testing for interactions between the two measures of Alzheimer pathology, we found an interaction between R_1 and BP_{ND} for slope of RAVLT immediate (beta$_{R1} \times_{BP} \times_{time}$ -0.23 (SE 0.09)), such that the effect of R_1 on RAVLT immediate slopes was mainly present in individuals with low BP_{ND}. There was no interaction for any of the other neuropsychological tests, implying independent effects on cognitive decline of BP_{ND} and R_1.

Table 2 Relationship between R_1, BP_{ND}, and cognition in composite region of interest

|	Concurrent				Longitudinal			
	Model 1	Model 2	Model 3		Model 1	Model 2	Model 3	
	R_1	BP_{ND}	R_1	BP_{ND}	$R_1 \times$ time	$BP_{ND} \times$ time	$R_1 \times$ time	$BP_{ND} \times$ time
VAT-A	-0.09 (0.05)	-0.07 (0.05)	-0.09 (0.05)	-0.07 (0.05)	0.01 (0.01)	-0.02 (0.01)	0.01 (0.01)	-0.02 (0.01)
RAVLT immediate	0.04 (0.59)	-0.77 (0.58)	0.05 (0.59)	-0.79 (0.59)	**0.27 (0.13)**	**-0.70 (0.12)***	**0.29 (0.11)*†**	**-0.70 (0.12)*†**
RAVLT delayed	0.01 (0.20)	**-0.41 (0.20)**	-0.0001 (0.20)	**-0.40 (0.20)**	**0.09 (0.04)**	**-0.24 (0.04)***	**0.08 (0.03)**	**-0.23 (0.04)***
Animal fluency	0.01 (0.36)	-0.41 (0.36)	0.04 (0.36)	-0.41 (0.36)	0.04 (0.05)	**-0.22 (0.06)***	0.04 (0.05)	**-0.22 (0.06)***
TMT-A	0.01 (0.02)	-0.01 (0.02)	0.01 (0.02)	-0.01 (0.02)	**0.01 (0.003)**	-0.01 (0.003)	**0.01 (0.003)**	-0.01 (0.003)
TMT-B	0.001 (0.02)	-0.03 (0.02)	0.002 (0.02)	-0.03 (0.02)	0.003 (0.003)	**-0.01 (0.003)**	0.003 (0.003)	**-0.01 (0.003)**
Stroop I	0.0001 (0.01)	-0.01 (0.01)	0.001 (0.01)	-0.01 (0.01)	0.002 (0.001)	**-0.004 (0.002)***	0.002 (0.001)	**-0.004 (0.002)***
Stroop II	0.0004 (0.01)	-0.01 (0.01)	0.0003 (0.01)	-0.01 (0.01)	0.002 (0.002)	**-0.01 (0.002)***	0.002 (0.002)	**-0.01 (0.002)***
Stroop III	-0.004 (0.01)	-0.002 (0.02)	-0.01 (0.01)	-0.002 (0.02)	-0.001 (0.003)	**-0.01 (0.003)***	-0.002 (0.003)	**-0.01 (0.003)***
MMSE	-0.08 (0.07)	**-0.21 (0.07)**	-0.08 (0.07)	**-0.21 (0.07)**	**0.04 (0.02)**	**-0.05 (0.02)**	0.04 (0.02)	**-0.05 (0.02)**

Values given are beta (SE) obtained via linear mixed models. Outcome: cognitive test performance. Predictors: Model 1: R_1, time, $R_1 \times$ time; Model 2: BP_{ND}, time, $BP_{ND} \times$ time; Model 3: R_1, BP_{ND}, time, $R_1 \times$ time, $BP_{ND} \times$ time. For all neuropsychological tests as outcome, we tested whether the interaction term $R_1 \times BP_{ND} \times$ time was significant. When this was the case, we show the betas of $R_1 \times$ time and $BP_{ND} \times$ time of the model that included this three-way interaction term. All models were corrected for age, sex, education, and PET and MRI scanner type. Betas reflect the association with annual decline (interaction between predictor and time). Models included a random intercept, and a random slope was added for RAVLT immediate, RAVLT delayed, Stroop II, Stroop III, and MMSE. TMT and Stroop were log transformed and inverted. R_1 and BP_{ND} are z-transformed

Bold p value < 0.05; *FDR corrected p value < 0.05

†interaction term $R_1 \times BP_{ND} \times$ time p value < 0.05

SE standard error, *VAT* Visual Association Test, *RAVLT* Rey Auditory Verbal Learning Task, *TMT* Trail Making Test, *MMSE* Mini-Mental State Examination

Fig. 1 Neuropsychological test performance over time. Spaghetti plots showing individual neuropsychological trajectories on two neuropsychological tests. Rey Auditory Verbal Learning Task delayed recall (**a** and **c**) and mini mental state examination (**b** and **d**). For visualization, the sample was divided into tertiles. Separate lines represent the unadjusted mean trajectory for each R_1 tertile separately (**a** and **b**, based on baseline R_1 values) and for each BP_{ND} tertile separately (**c** and **d**, based on baseline BP_{ND} values). Figures represent raw test scores
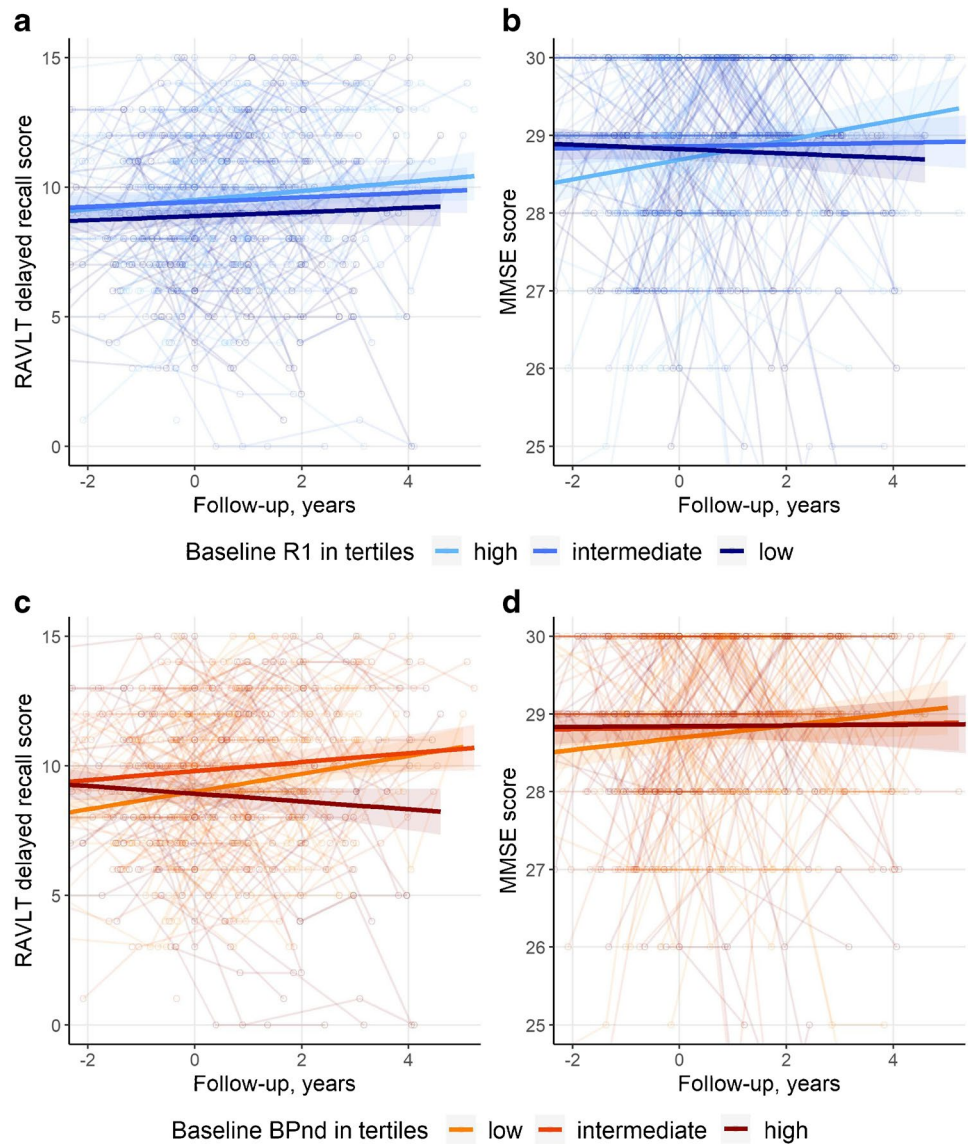
Relationship between BP_{ND} and R_1

Next, we investigated the relationship between BP_{ND} and R_1. We first investigated the effect of BP_{ND} on R_1 (Table 3). Somewhat counterintuitively, higher baseline values for occipital BP_{ND} were associated with higher baseline values for occipital R_1 (Table 3). There were no cross-sectional associations in other regions. By contrast, longitudinally, in all regions higher baseline BP_{ND} was associated with steeper decrease in R_1 in those same regions. All associations between baseline BP_{ND} and R_1 longitudinal trajectories remained significant after correction for multiple testing. Figure 2 visualizes the association between baseline BP_{ND} and R_1 over time.

Next, we investigated the effect of R_1 on BP_{ND} (Table 4). Again, we found higher baseline values for occipital R_1 to be associated with higher concurrent values for occipital BP_{ND},

but no cross-sectional associations in other regions. Longitudinally, baseline R_1 values in frontal, temporal, and composite regions were inversely associated with change in BP_{ND} over time in those same regions. This means a lower baseline R_1 was associated with an increase in BP_{ND} over time. After correction for multiple testing, baseline R_1 remained associated with longitudinal BP_{ND} in frontal and composite regions. Figure 3 visualizes the association between baseline R_1 and BP_{ND} over time.

Discussion

In this study in a relatively large sample of cognitively normal individuals, we found that low rCBF and high amyloid burden, both measured by dynamic [18F]florbetapir PET, were independently associated with worse trajectories

Table 3 Associations with cross-sectional and longitudinal R_1

	Region	Concurrent	Longitudinal
Model 1	Frontal	0.08 (0.07)	**− 0.08 (0.03)***
	Temporal	− 0.07 (0.07)	**− 0.12 (0.03)***
	Parietal	− 0.03 (0.07)	**− 0.09 (0.03)***
	Occipital	0.14 (0.08)	**− 0.12 (0.04)***
	Composite	− 0.07 (0.07)	**− 0.11 (0.03)***
Model 2	Frontal	0.08 (0.07)	**− 0.09 (0.03)***
	Temporal	0.01 (0.07)	**− 0.12 (0.03)***
	Parietal	0.03 (0.07)	**− 0.10 (0.03)***
	Occipital	**0.15 (0.08)**	**− 0.14 (0.04)***
	Composite	− 0.003 (0.07)	**− 0.11 (0.03)***

Results shown are beta (SE) as estimated by linear mixed models, outcome is R_1. In model 1, the predictors are BP_{ND}, time between PET scans in years, and the interaction $BP_{ND} \times$ time. Model 2 is additionally corrected for age, sex, and PET and MRI scanner type. Values given represent betas associated with BP_{ND} (concurrent) and $BP_{ND} \times$ time (longitudinal). Models included a random intercept. R_1 and BP_{ND} are z-transformed

Bold p value < 0.05. *FDR corrected p value < 0.05

for tests of memory and attention. Longitudinal imaging showed that despite the absence of cross-sectional associations, higher baseline amyloid burden was associated with a decline in rCBF over time, while at the same time, a low baseline rCBF was associated with increase in amyloid burden over time. This provides evidence that amyloid accumulation and reduced rCBF are parallel disease processes without fixed order in the cascade of events leading to cognitive decline.

We found that low baseline rCBF predicted worse performance over time on tests for memory and attention. After adding baseline amyloid burden as covariate, rCBF remained associated with cognitive slope. For one memory test, there seemed to be an interaction effect, as rCBF predicted cognitive slope mainly in individuals with low amyloid burden. Our results are in line with previous studies that showed low baseline CBF predicted future cognitive decline [23, 24], and clinical progression to MCI or dementia [38, 39]. We extend on these findings by showing rCBF adds unique predictive value in addition to amyloid burden, using an extensive neuropsychological test battery. Previous studies with a cross-sectional design found that lower baseline CBF was associated with worse concurrent cognitive performance in the entire disease spectrum [9, 11, 14, 40], but studies specifically investigating cognitively normal individuals report conflicting results [20, 22]. We did not find any cross-sectional associations between baseline rCBF and cognition. This is probably due to the fact that to be included in the SCIENCe project, our participants were extensively tested and judged to be cognitively normal, so variability in cognition at baseline is limited. This further highlights the

importance of a longitudinal design with sufficient follow-up to study how brain changes contribute to cognitive decline in the earliest disease stages.

When we evaluated rCBF and amyloid burden longitudinally, the two measures were clearly associated, as high baseline amyloid burden was associated with a decline in rCBF, while vice versa and contrary to our hypotheses, a low baseline rCBF was also associated with an increase in amyloid burden. There are a number of possible explanations for these observations. According to the amyloid cascade hypothesis, and as translated to living humans in the hypothetical biomarker model, amyloid accumulation is among the first changes related to AD. This subsequently leads to tau deposition and then to neuronal injury. When we interpret rCBF as a measure of neuronal injury, we would expect to observe reduced rCBF downstream of amyloid. Our observation that high baseline amyloid burden predisposes for decline over time in rCBF is in line with this hypothesis [1]. They are also in line with studies suggesting low CBF to reflect decreases in metabolism and synaptic failure, because this places a decreasing CBF towards the end of the pathophysiology of AD [7, 8]. However, we also found low rCBF values in individuals with low amyloid burden, associated with subsequent increase in amyloid burden. This does not fit within this hypothetical sequence. Alternative hypotheses on the origin of AD include the two-hit vascular hypothesis, which poses that damage to the microcirculation of the brain resulting from vascular risk factors (hit one) would lead to reduced CBF [6, 41]. The compromised vessels would than lead to suboptimal breakdown and clearance of amyloid, which would result in amyloid accumulation (hit two). In this scenario, amyloid accumulation would be a downstream effect of reduced CBF. Our second observation, that low baseline rCBF also predisposes for an increase in amyloid burden over time, is in line with this second hypothesis. The probabilistic model of AD recognizes three variants of the disease and highlights that AD is a very complex disease and many factors are related to cognitive decline [42]. To add to this complexity, neurodegenerative pathologies other than AD are also related to cognitive decline. In our sample, one individual showed clinical progression to dementia with Lewy bodies and another to vascular dementia. Furthermore, mixed pathologies in neurodegenerative disease are not uncommon. For example, AD pathology is seen frequently in combination with alpha-synuclein inclusions, or vascular pathology [43]. Therefore, pathologies other than AD could also have contributed to our results. Overall, our results provide evidence for different sequences of events, and show that different factors contribute to cognitive decline, which underlines the complexity of cognitive decline.

In contrast to our longitudinal findings, we did not find cross-sectional associations between rCBF and amyloid burden, except in the occipital region, in which a higher amyloid
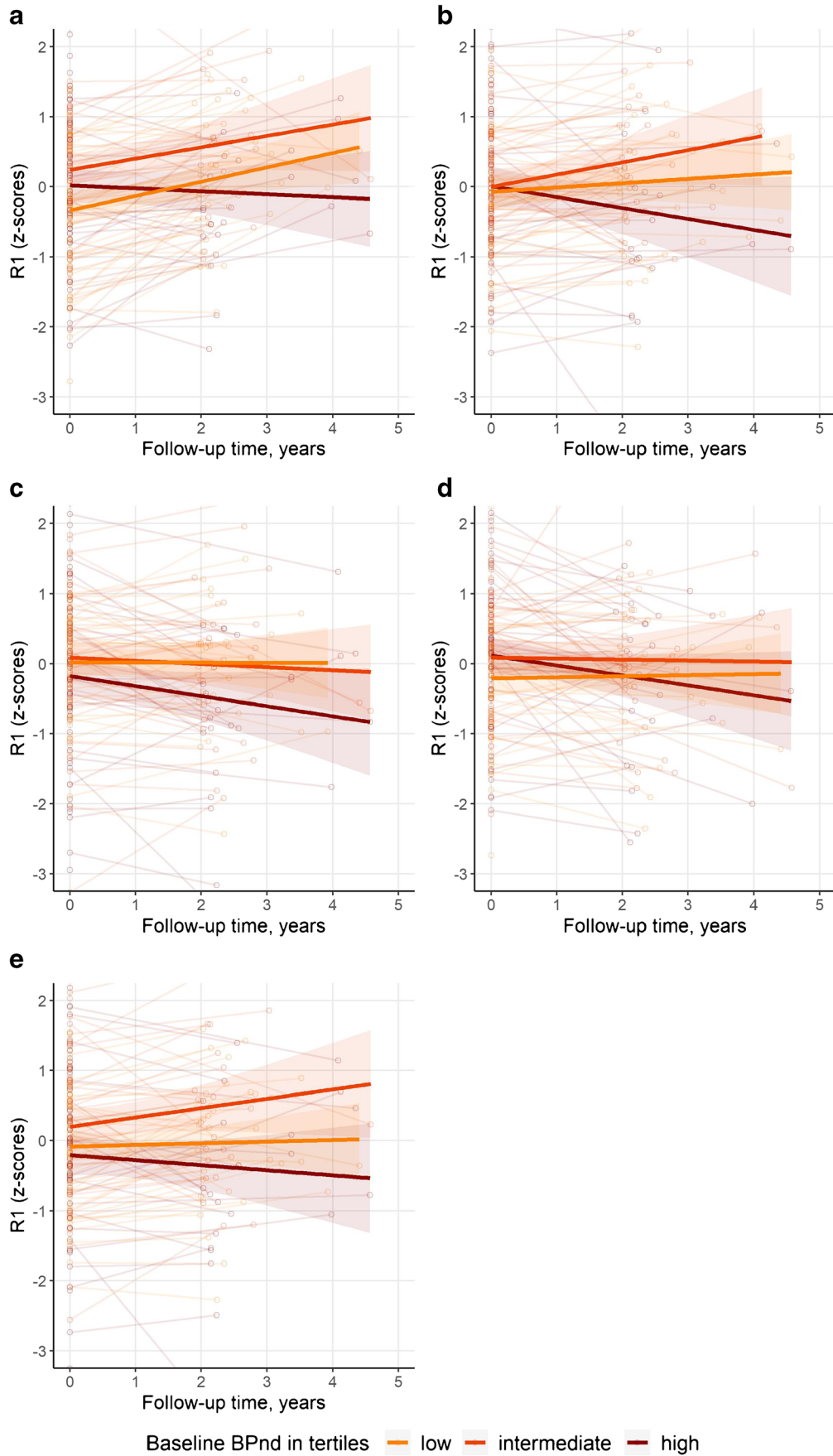
◀**Fig. 2** Visualization of trajectories of R_1 over time. Spaghetti plots showing individual trajectories of R_1 over time (**a** Frontal, **b** Temporal, **c** Parietal, **d** Occipital, **e** Composite regions). For visualization, the sample was divided into tertiles. Separate lines represent BP_{ND} tertiles (based on baseline values). BP_{ND} and R_1 are z-transformed

burden was subtly associated with a higher rCBF. This might be interpreted as overcompensation, yet we feel that this result should not be overinterpreted, since the association did not survive correction for multiple testing. Previous studies in cognitively normal individuals found contradictory results. Some found lower CBF in amyloid positive individuals [18], others a higher CBF [15], or no amyloid-related differences in CBF at all [20, 21]. The lack of cross-sectional associations in our sample of cognitively normal individuals, in combination with the inconsistencies in literature, highlights the importance of longitudinal data to study how different measures of brain pathology contribute to cognitive decline and dementia. Pathology accumulates in the course of many years, and this further stresses the relevance of well-phenotyped clinical cohorts with sufficiently long duration of follow-up.

Our study is among the first to investigate the longitudinal relationships between amyloid burden and rCBF. Only one other study in 28 nondemented elderly investigated change in CBF using $[^{15}O]H_2O$ PET in relation to amyloid status, and found both increases and decreases in CBF in amyloid-positive individuals compared to amyloid-negative individuals [16], This study concluded that the decrease in CBF in amyloid-positive individuals represented a response to neuronal insult as a result of amyloid deposition, providing evidence for the theory that amyloid accumulation predisposes for a reduction in CBF. They interpreted the increases as a representation of a compensational effect by attempting to preserve neuronal function. The latter could be viewed in line with our cross-sectional finding of a high amyloid burden related to a high rCBF in the occipital region. However, we feel that this result should not be overinterpreted. Furthermore, there are a number of differences with our study. First, this study investigated CBF but not amyloid deposition longitudinally. Also, this study acquired images for 60 s once the total radioactivity counts in the brain reached threshold levels. This is a semi-quantitative method for analysis of $[^{15}O]H_2O$ PET data, which may have compromised the CBF measurements. Last, we used a much larger sample size, which makes our results more robust.

Our study has important implications. We show that amyloid accumulation and reduction in rCBF are separate and parallel disease processes which independently contribute to cognitive decline while influencing each other longitudinally, without ordering one process before the

other. This provides additional insight in the pathophysiology of AD. Our results suggest that in the hypothetical biomarker model of amyloid accumulation leading to tau pathology, neuronal injury, and cognitive decline, changes in CBF could be placed before or after amyloid accumulation. Since other studies also show tau pathology and rCBF are independently associated with cognition in AD, rCBF probably reflects a different aspect of AD pathology [44]. It furthermore illustrates there are multiple pathways through which AD biomarkers can become abnormal.

Strengths of our study include that we had a relatively large sample of cognitively normal individuals with considerable follow-up. We show that by using one dynamic $[^{18}F]$florbetapir PET scan, information about two relevant biomarkers can be obtained, which both provide predictive information about future cognitive decline. Additionally, we had repeated PET scans available for a large group of participants, enabling the investigation of longitudinal trajectories of rCBF and amyloid burden. Limitations of our study include that we did not take all variables into account that potentially affect rCBF, such as diurnal variations, genetic factors, and cerebrovascular risk factors. Last, although we already had a relatively long follow-up duration of 3.8 years on average, an even longer period would enable us to capture more clinically relevant changes in cognition, in this sample of cognitively normal individuals.

Concluding, we showed that amyloid burden and rCBF were independently associated with cognitive decline over

Table 4 Associations with cross-sectional and longitudinal BP_{ND}

	Region	Concurrent	Longitudinal
Model 1	Frontal	0.09 (0.07)	**− 0.08 (0.02)***
	Temporal	− 0.06 (0.07)	**− 0.03 (0.01)**
	Parietal	− 0.01 (0.07)	− 0.02 (0.01)
	Occipital	**0.14 (0.07)**	0.0003 (0.02)
	Composite	− 0.06 (0.07)	**− 0.04 (0.01)***
Model 2	Frontal	0.09 (0.08)	**− 0.08 (0.02)***
	Temporal	0.04 (0.08)	**− 0.03 (0.01)**
	Parietal	0.05 (0.08)	− 0.02 (0.01)
	Occipital	**0.18 (0.08)**	− 0.002 (0.02)
	Composite	0.02 (0.08)	**− 0.04 (0.01)***

Results shown are beta (SE) as estimated by linear mixed models, outcome is BP_{ND}. In model 1, the predictors are R_1, time between PET scans in years, and the interaction $R_1 \times$ time. Model 2 is additionally corrected for age, sex, and PET and MRI scanner type. Values given represent beta associated with R_1 (concurrent) and $R_1 \times$ time (longitudinal). Models included a random intercept. R_1 and BP_{ND} are z-transformed

Bold p value < 0.05. *FDR corrected p value < 0.05

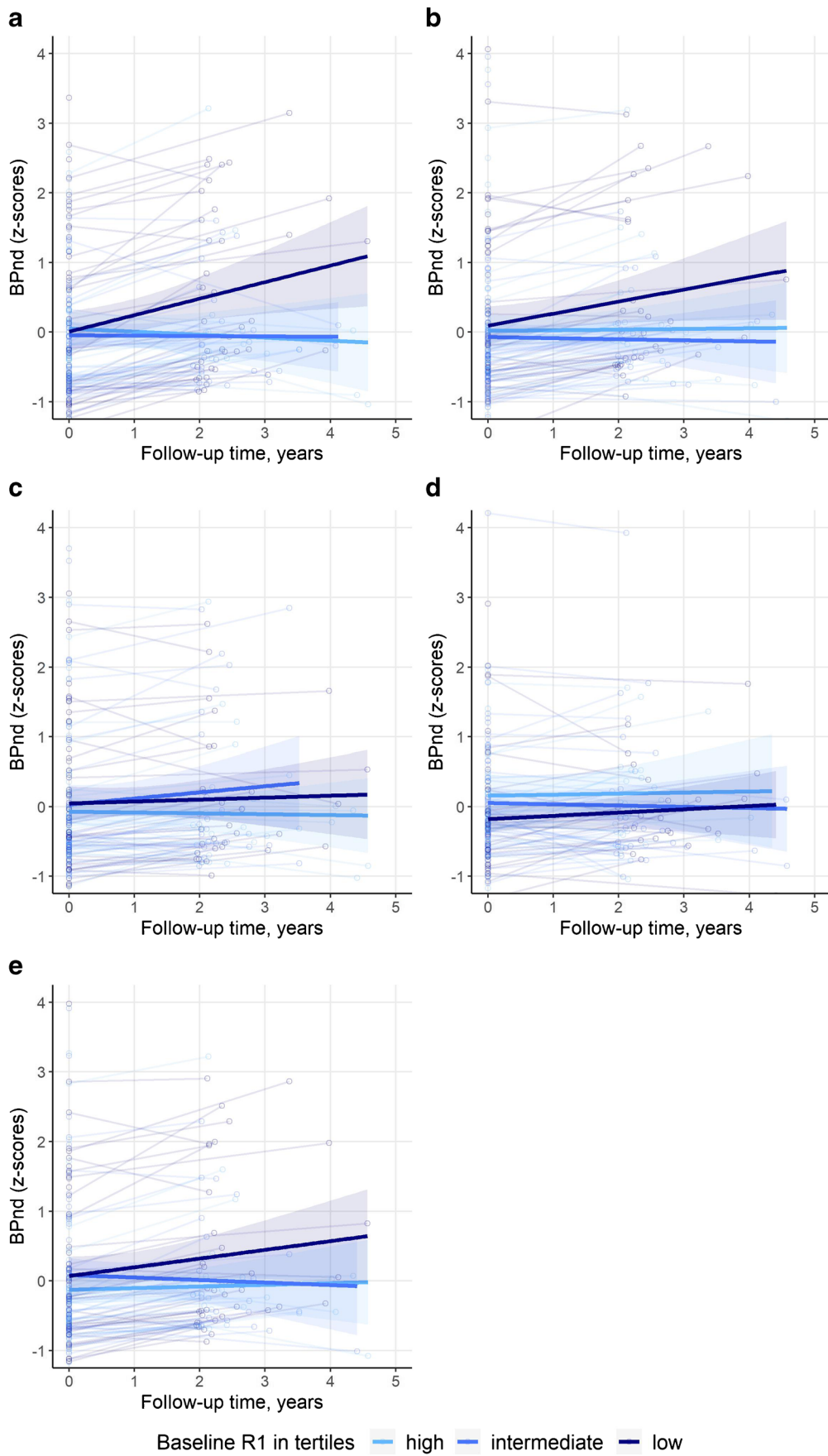**◄Fig. 3** Visualization of trajectories of BP_{ND} over time. Spaghetti plots showing individual trajectories of BP_{ND} over time (**a** Frontal, **b** Temporal, **c** Parietal, **d** Occipital, **e** Composite regions). For visualization, the sample was divided into tertiles. Separate lines represent R_1 tertiles (based on baseline values). BP_{ND} and R_1 are z-transformed

time in a group of initially cognitively normal individuals. Even though there were hardly any cross-sectional relationships between amyloid burden and rCBF, we observed an association between high baseline amyloid burden and a subsequent decrease in rCBF, and inversely an association between a low baseline rCBF and a subsequent increase in amyloid burden. Our results provide evidence that amyloid accumulation and decrease of CBF are separate and parallel disease processes, each of them providing unique predictive information, and enhancing the other longitudinally.

Data availability The data that support the findings of this study may be shared upon reasonable request.

Declarations

Ethics approval The study was approved by the medical ethical committee of the VU University and was in accordance with the Helsinki Declaration of 1975.

Consent to participate All participants gave written informed consent.

Competing interests Jarith Ebenau reports no disclosures relevant to the manuscript.

Denise Visser reports no disclosures relevant to the manuscript.
Sander Verfaillie reports no disclosures relevant to the manuscript.
Tessa Timmers reports no disclosures relevant to the manuscript.
Mardou van Leeuwenstijn reports no disclosures relevant to the manuscript.
Mara ten Kate reports no disclosures relevant to the manuscript.
Frederik Barkhof is a consultant for Biogen-Idec, Bayer-Schering, Merck-Serono, Roche, NovartisIXICO, and Combinostics; has received sponsoring from European Commission-Horizon 2020, National Institute for Health Research-University College London Hospitals Bio-

medical Research Centre, TEVA, Novartis, and Biogen; and serves on the editorial boards of *Radiology*, *Brain*, *Neuroradiology*, *Multiple Sclerosis Journal*, and *Neurology*.
Philip Scheltens has acquired grant support (for the institution) from Biogen. In the past two years, he has received consultancy/speaker fees (paid to the institution) from Probiodrug Biogen, EIP Pharma, Merck AG.
Niels Prins is consultant to Boehringer Ingelheim, Aribio, and Amylyx. He is co-PI of a study with Fuji Film Toyama Chemical. He serves on the DSMB of Abbvie's M15-566 trial. NP has received a speaker fee from Biogen. Payments were made to his company. He is CEO and co-owner of the Brain Research Centre, The Netherlands.
Ronald Boellaard reports no disclosures relevant to the manuscript.
Bert Windhorst reports no disclosures relevant to the manuscript.
Wiesje van der Flier Research programs have been funded by ZonMW, NWO, EU-FP7, EU-JPND, Alzheimer Nederland, CardioVascular Onderzoek Nederland, Health ~ Holland, Topsector Life Sciences & Health, stichting Dioraphte, Gieskes-Strijbis fonds, stichting Equilibrio, Pasman stichting, Biogen MA Inc, Boehringer Ingelheim, Life-MI, AVID, Roche BV, Fujifilm, Combinostics. WF is recipient of a grant for the Heart-Brain Connection crossroads (HBCx) consortium of the Dutch CardioVascular Alliance (DCVA). This work was supported by the Dutch Heart Foundation [#2018–28]. WF holds the Pasman chair. WF has performed contract research for Biogen MA Inc and Boehringer Ingelheim. WF has been an invited speaker at Boehringer Ingelheim, Biogen MA Inc, Danone, Eisai and WebMD Neurology (Medscape). WF is consultant to Oxford Health Policy Forum CIC, Roche, and Biogen MA Inc. WF was associate editor at *Alzheimer's Research & Therapy* (2020–2021); She is associate editor of *Brain* (2021–). All funding is paid to her institution.
Bart van Berckel has received research support from EU-FP7, CTMM, ZonMw, NWO, and Alzheimer Nederland. BvB has performed contract research for Rodin, IONIS, AVID, Eli Lilly, UCB, DIAN-TUI, and Janssen. BvB was a speaker at a symposium organized by Springer Healthcare. BvB has a consultancy agreement with IXICO for the reading of PET scans. BvB is a trainer for GE. BvB only receives financial compensation from Amsterdam UMC.

References

1. Jack CR, Bennett DA, Blennow K, Carrillo MC, Dunn B, Haeberlein SB, et al. NIA-AA Research Framework: Toward a biological definition of Alzheimer's disease. Alzheimers Dement. 2018;14:535–62. https://doi.org/10.1016/j.jalz.2018.02.018.
2. Baker JE, Lim YY, Pietrzak RH, Hassenstab J, Snyder PJ, Masters CL, et al. Cognitive impairment and decline in cognitively normal older adults with high amyloid-β: A meta-analysis. Alzheimers Dement: Diagn Assess Dis Monit. 2017;6:108–21. https://doi.org/10.1016/j.dadm.2016.09.002.

3. Hardy J, Selkoe DJ. The amyloid hypothesis of Alzheimer's disease: Progress and problems on the road to therapeutics. Science (New York, NY). 2002;297:353–6. https://doi.org/10.1126/science.1072994.

4. Leng F, Edison P. Neuroinflammation and microglial activation in Alzheimer disease: Where do we go from here? Nat Rev Neurol. 2021;17:157–72. https://doi.org/10.1038/s41582-020-00435-y.

5. Jansen WJ, Ossenkoppele R, Knol DL, Tijms BM, Scheltens P, Verhey FR, et al. Prevalence of cerebral amyloid pathology in persons without dementia: A meta-analysis. JAMA. 2015;313:1924–38. https://doi.org/10.1001/jama.2015.4668.

6. Zlokovic BV. Neurovascular pathways to neurodegeneration in Alzheimer's disease and other disorders. Nat Rev Neurosci. 2011;12:723–38. https://doi.org/10.1038/nrn3114.

7. Chen Y, Wolk DA, Reddin JS, Korczykowski M, Martinez PM, Musiek ES, et al. Voxel-level comparison of arterial spin-labeled perfusion MRI and FDG-PET in Alzheimer disease. Neurology. 2011;77:1977–85. https://doi.org/10.1212/WNL.0b013e31823a0ef7.

8. Musiek ES, Chen Y, Korczykowski M, Saboury B, Martinez PM, Reddin JS, et al. Direct comparison of fluorodeoxyglucose positron emission tomography and arterial spin labeling magnetic resonance imaging in Alzheimer's disease. Alzheimers Dement: J Alzheimers Assoc. 2012;8:51–9. https://doi.org/10.1016/j.jalz.2011.06.003.

9. Duan W, Sehrawat P, Balachandrasekaran A, Bhumkar AB, Boraste PB, Becker JT, et al. Cerebral blood flow is associated with diagnostic class and cognitive decline in Alzheimer's disease. J Alzheimers Dis: JAD. 2020;76:1103–20. https://doi.org/10.3233/jad-200034.

10. Ottoy J, Verhaeghe J, Niemantsverdriet E, De Roeck E, Wyffels L, Ceyssens S, et al. (18)F-FDG PET, the early phases and the delivery rate of (18)F-AV45 PET as proxies of cerebral blood flow in Alzheimer's disease: Validation against (15)O-H2O PET. Alzheimers Dement: J Alzheimers Assoc. 2019. https://doi.org/10.1016/j.jalz.2019.05.010.

11. de Eulate RG, Goñi I, Galiano A, Vidorreta M, Recio M, Riverol M, et al. Reduced cerebral blood flow in mild cognitive impairment assessed using phase-contrast MRI. J Alzheimers Dis: JAD. 2017;58:585–95. https://doi.org/10.3233/jad-161222.

12. Michels L, Warnock G, Buck A, Macauda G, Leh SE, Kaelin AM, et al. Arterial spin labeling imaging reveals widespread and Aβ-independent reductions in cerebral blood flow in elderly apolipoprotein epsilon-4 carriers. J Cereb Blood Flow Metab: Off J Int Soc Cereb Blood Flow Metab. 2016;36:581–95. https://doi.org/10.1177/0271678x15605847.

13. Gietl AF, Warnock G, Riese F, Kälin AM, Saake A, Gruber E, et al. Regional cerebral blood flow estimated by early PiB uptake is reduced in mild cognitive impairment and associated with age in an amyloid-dependent manner. Neurobiol Aging. 2015;36:1619–28. https://doi.org/10.1016/j.neurobiolaging.2014.12.036.

14. Leijenaar JF, van Maurik IS, Kuijer JPA, van der Flier WM, Scheltens P, Barkhof F, et al. Lower cerebral blood flow in subjects with Alzheimer's dementia, mild cognitive impairment, and subjective cognitive decline using two-dimensional phase-contrast magnetic resonance imaging. Alzheimers Dement (Amsterdam, Netherlands). 2017;9:76–83. https://doi.org/10.1016/j.dadm.2017.10.001.

15. Fazlollahi A, Calamante F, Liang X, Bourgeat P, Raniga P, Dore V, et al. Increased cerebral blood flow with increased amyloid burden in the preclinical phase of Alzheimer's disease. J Magn Reson Imaging: JMRI. 2020;51:505–13. https://doi.org/10.1002/jmri.26810.

16. Sojkova J, Beason-Held L, Zhou Y, An Y, Kraut MA, Ye W, et al. Longitudinal cerebral blood flow and amyloid deposition: an emerging pattern? J Nucl Med: Off Publ Soc Nucl Med. 2008;49:1465–71. https://doi.org/10.2967/jnumed.108.051946.

17. Mattsson N, Tosun D, Insel PS, Simonson A, Jack CR Jr, Beckett LA, et al. Association of brain amyloid-β with cerebral perfusion and structure in Alzheimer's disease and mild cognitive impairment. Brain J Neurol. 2014;137:1550–61. https://doi.org/10.1093/brain/awu043.

18. Bilgel M, Beason-Held L, An Y, Zhou Y, Wong DF, Resnick SM. Longitudinal evaluation of surrogates of regional cerebral blood flow computed from dynamic amyloid PET imaging. J Cereb Blood Flow Metab: Off J Int Soc Cereb Blood Flow Metab. 2020;40:288–97. https://doi.org/10.1177/0271678x19830537.

19. Albrecht D, Isenberg AL, Stradford J, Monreal T, Sagare A, Pachicano M, et al. Associations between vascular function and Tau PET are associated with global cognition and amyloid. J Neurosci: Off J Soc Neurosci. 2020;40:8573–86. https://doi.org/10.1523/jneurosci.1230-20.2020.

20. Bangen KJ, Clark AL, Edmonds EC, Evangelista ND, Werhane ML, Thomas KR, et al. Cerebral blood flow and amyloid-β interact to affect memory performance in cognitively normal older adults. Front Aging Neurosci. 2017;9:181. https://doi.org/10.3389/fnagi.2017.00181.

21. Funaki K, Nakajima S, Noda Y, Wake T, Ito D, Yamagata B, et al. Can we predict amyloid deposition by objective cognition and regional cerebral blood flow in patients with subjective cognitive decline? Psychogeriatr Off J Japan Psychogeriatr Soc. 2019;19:325–32. https://doi.org/10.1111/psyg.12397.

22. Staffaroni AM, Cobigo Y, Elahi FM, Casaletto KB, Walters SM, Wolf A, et al. A longitudinal characterization of perfusion in the aging brain and associations with cognition and neural structure. Hum Brain Mapp. 2019;40:3522–33. https://doi.org/10.1002/hbm.24613.

23. Benedictus MR, Leeuwis AE, Binnewijzend MA, Kuijer JP, Scheltens P, Barkhof F, et al. Lower cerebral blood flow is associated with faster cognitive decline in Alzheimer's disease. Eur Radiol. 2017;27:1169–75. https://doi.org/10.1007/s00330-016-4450-z.

24. De Vis JB, Peng SL, Chen X, Li Y, Liu P, Sur S, et al. Arterial-spin-labeling (ASL) perfusion MRI predicts cognitive function in elderly individuals: A 4-year longitudinal study. J Magn Reson Imaging: JMRI. 2018;48:449–58. https://doi.org/10.1002/jmri.25938.

25. Golla SS, Verfaillie SC, Boellaard R, Adriaanse SM, Zwan MD, Schuit RC, et al. Quantification of [(18)F]florbetapir: A test-retest tracer kinetic modelling study. J Cereb Blood Flow Metab: Off J Int Soc Cereb Blood Flow Metab. 2019;39:2172–80. https://doi.org/10.1177/0271678x18783628.

26. Meyer PT, Hellwig S, Amtage F, Rottenburger C, Sahm U, Reuland P, et al. Dual-biomarker imaging of regional cerebral amyloid load and neuronal activity in dementia with PET and 11C-labeled Pittsburgh compound B. J Nucl Med: Off Publ Soc Nucl Med. 2011;52:393–400. https://doi.org/10.2967/jnumed.110.083683.

27. Hays CC, Zlatar ZZ, Wierenga CE. The utility of cerebral blood flow as a biomarker of preclinical Alzheimer's disease. Cell Mol Neurobiol. 2016;36:167–79. https://doi.org/10.1007/s10571-015-0261-z.

28. Slot RER, Verfaillie SCJ, Overbeek JM, Timmers T, Wesselman LMP, Teunissen CE, et al. Subjective cognitive impairment cohort (SCIENCe): Study design and first results. Alzheimers Res Ther. 2018;10:76. https://doi.org/10.1186/s13195-018-0390-y.

29. van der Flier WM, Scheltens P. Amsterdam dementia cohort: Performing research to optimize care. J Alzheimers Dis: JAD. 2018;62:1091–111. https://doi.org/10.3233/jad-170850.

30. van der Flier WM, Pijnenburg YA, Prins N, Lemstra AW, Bouwman FH, Teunissen CE, et al. Optimizing patient care and

research: The Amsterdam Dementia Cohort. J Alzheimers Dis: JAD. 2014;41:313–27. https://doi.org/10.3233/jad-132306.

31. Hammers A, Allom R, Koepp MJ, Free SL, Myers R, Lemieux L, et al. Three-dimensional maximum probability atlas of the human brain, with particular reference to the temporal lobe. Hum Brain Mapp. 2003;19:224–47. https://doi.org/10.1002/hbm.10123.

32. Lammertsma AA. Forward to the past: The case for quantitative PET imaging. J Nucl Med: Off Publ Soc Nucl Med. 2017;58:1019–24. https://doi.org/10.2967/jnumed.116.188029.

33. Gunn RN, Lammertsma AA, Hume SP, Cunningham VJ. Parametric imaging of ligand-receptor binding in PET using a simplified reference region model. Neuroimage. 1997;6:279–87. https://doi.org/10.1006/nimg.1997.0303.

34. Verfaillie SCJ, Golla SSV, Timmers T, Tuncel H, van der Weijden CWJ, Schober P et al. Repeatability of parametric methods for [18F]florbetapir imaging in Alzheimer's disease and healthy controls: A test–retest study. J Cereb Blood Flow Metab. 2020; 0271678X20915403. https://doi.org/10.1177/0271678X20915403.

35. Joshi AD, Pontecorvo MJ, Lu M, Skovronsky DM, Mintun MA, Devous MD Sr. A Semiautomated method for quantification of F 18 Florbetapir PET Images. J Nucl Med: Off Publ Soc Nucl Med. 2015;56:1736–41. https://doi.org/10.2967/jnumed.114.153494.

36. Fazekas F, Chawluk JB, Alavi A, Hurtig HI, Zimmerman RA. MR signal abnormalities at 1.5 T in Alzheimer's dementia and normal aging. AJR Am J Roentgenol. 1987;149:351–6. https://doi.org/10.2214/ajr.149.2.351.

37. Timmers T, Ossenkoppele R, Verfaillie SCJ, van der Weijden CWJ, Slot RER, Wesselman LMP, et al. Amyloid PET and cognitive decline in cognitively normal individuals: The SCIENCe project. Neurobiol Aging. 2019;79:50–8. https://doi.org/10.1016/j.neurobiolaging.2019.02.020.

38. Park KW, Yoon HJ, Kang DY, Kim BC, Kim S, Kim JW. Regional cerebral blood flow differences in patients with mild cognitive impairment between those who did and did not develop Alzheimer's disease. Psychiatry Res. 2012;203:201–6. https://doi.org/10.1016/j.pscychresns.2011.12.007.

39. Wolters FJ, Zonneveld HI, Hofman A, van der Lugt A, Koudstaal PJ, Vernooij MW, et al. Cerebral perfusion and the risk of dementia: A population-based study. Circulation. 2017;136:719–28. https://doi.org/10.1161/circulationaha.117.027448.

40. Leeuwis AE, Benedictus MR, Kuijer JPA, Binnewijzend MAA, Hooghiemstra AM, Verfaillie SCJ, et al. Lower cerebral blood flow is associated with impairment in multiple cognitive domains in Alzheimer's disease. Alzheimers Dement: J Alzheimers Assoc. 2017;13:531–40. https://doi.org/10.1016/j.jalz.2016.08.013.

41. Korte N, Nortley R, Attwell D. Cerebral blood flow decrease as an early pathological mechanism in Alzheimer's disease. Acta Neuropathol. 2020;140:793–810. https://doi.org/10.1007/s00401-020-02215-w.

42. Frisoni GB, Altomare D, Thal DR, Ribaldi F, van der Kant R, Ossenkoppele R, et al. The probabilistic model of Alzheimer disease: The amyloid hypothesis revised. Nat Rev Neurosci. 2022;23:53–66. https://doi.org/10.1038/s41583-021-00533-w.

43. Matej R, Tesar A, Rusina R. Alzheimer's disease and other neurodegenerative dementias in comorbidity: A clinical and neuropathological overview. Clin Biochem. 2019;73:26–31. https://doi.org/10.1016/j.clinbiochem.2019.08.005.

44. Visser D, Wolters EE, Verfaillie SCJ, Coomans EM, Timmers T, Tuncel H, et al. Tau pathology and relative cerebral blood flow are independently associated with cognition in Alzheimer's disease. Eur J Nucl Med Mol Imaging. 2020;47:3165–75. https://doi.org/10.1007/s00259-020-04831-w.